



Thermoluminescent Response of Ce- and Li-Doped CaF₂ Phosphor to Gamma and UV Irradiation

Nilo F. Cano¹ · Ruben R. M. Aquepucho² · Jessica Mosqueira-Yauri² · Klinton V. Turpo-Huahasoncco² · René R. Rocca¹ · J. F. Benavente³ · L. M. Rondan-Flores⁴ · J. F. D. Chubaci⁵ · Jorge S. Ayala-Arenas²

Received: 14 April 2024 / Accepted: 13 June 2024 / Published online: 26 June 2024
© The Author(s) under exclusive licence to Sociedade Brasileira de Física 2024

Abstract

In this work, Ce- and Li-doped CaF₂ phosphor (CaF₂:Ce,Li) was synthesized by the combustion technique. Structural and morphological analysis of the synthesized material has been carried out by X-ray diffraction (XRD) and scanning electron microscopy (SEM), respectively. The XRD pattern reveals the formation of a pure phase of the CaF₂ crystal with a crystal-lite size of 717 nm. The luminescence properties were investigated by the thermoluminescence (TL) technique. The effect of sintering temperature on the TL glow curve of the pellets has been investigated for different temperatures (450, 500, 525, 550, and 575 °C). Pellets sintered at 525 °C and 550 °C presented higher sensitivity in their TL responses for gamma and UV irradiation, respectively. Samples irradiated with gamma radiation show two intense TL peaks centered at 172 °C and 275 °C. On the other hand, samples irradiated with UV radiation show two peaks centered at 195 and 280 °C. The intensity of the TL peaks increases with gamma radiation dose and UV irradiation time. The kinetic parameters of the glow curve peaks were determined through the combined analysis of the results obtained by the Tm-Tstop and deconvolution methods.

Keywords CaF₂ phosphor · Thermoluminescence · Gamma irradiation · UV irradiation

1 Introduction

Exposure to ionizing and non-ionizing radiation (UV radiation) from natural sources (natural radioactive isotopes) as well as artificial sources used in various applications such as medical diagnostics, radiotherapy procedures, electricity generation (nuclear power plants), and applications in industry and research centers has increased considerably over the years. Therefore, it is important to predict or limit the effect

of radiation on living organisms, since ionizing radiation can cause the breaking of chemical bonds and the production of free radicals, among others.

These physical processes can, in turn, cause biological effects, including an increased risk of cancer development, cell death, tissue damage, and failure of vital organs, and consequently can lead to the death of the individual due to overexposure to radiation [1].

Paradoxically, the effects of radiation ionizing and non-ionizing radiation can also be beneficial, for example, radiation-induced cell death within a cancerous tumor is the basis for radiation therapy. Other applications of radiation are imaging in radiodiagnostics, radiation treatment for sterilization, food irradiation, polymer modification, etc. [1]. Therefore, different authors have been researching new materials for applications in ionizing radiation dosimetry with increasingly sensitive, stable, reproducible, and above all, precise responses.

Among radiation meters, solid-state passive luminescent dosimeters are the most widely used. These dosimeters measure the dose through the absorption of ionizing radiation energy and then emit this energy in the form of light. The quantification of the emitted light is performed based on thermoluminescence (TL) phenomena.

✉ Nilo F. Cano
nilo.cano@unifesp.br

Ruben R. M. Aquepucho
rmollohuanca@unsa.edu.pe

Jessica Mosqueira-Yauri
jmosqueira@unsa.edu.pe

¹ Universidade Federal de São Paulo - UNIFESP, Instituto Do Mar, Santos, SP, Brazil

² Universidad Nacional de San Agustín de Arequipa - UNSA, Arequipa, Peru

³ CIEMAT, Av. Complutense 40, e, 28040 Madrid, Spain

⁴ Instituto Pesquisas Energéticas e Nucleares, IPEN, CNEN/SP, São Paulo, SP, Brazil

⁵ Instituto de Física, Universidade de São Paulo, São Paulo, SP, Brazil

The mechanism that TL dosimeters use to quantify radiation is the deposition of ionizing radiation energy, which is directly related to the structural composition of the dosimetric material. The crystalline structure and defect centers responsible for the TL property of a material can be controlled by the proper choice of chemical reagents and synthesis route, so it is important to know the relationship between the chemical reagents and the preparation method.

Recent studies show that calcium fluoride (CaF_2) doped with rare earths and transition metals ($\text{CaF}_2:\text{Dy}$; $\text{CaF}_2:\text{Ce,Nd}$; $\text{CaF}_2:\text{Mn}$; $\text{CaF}_2:\text{Cu}$; $\text{CaF}_2:\text{Dy,Pb,Na}$; and $\text{CaF}_2:\text{Tm}$) [2–8], either divalent or trivalent, has important luminescent characteristics and important applications. These materials present high chemical stability, resistance to irradiation, and good emission in the visible region. Furthermore, it is known that CaF_2 is very sensitive to beta radiation [9–11], X rays [12], UV radiation [13], gamma radiation [14], and low energy ion [15]. On the other hand, natural calcium fluoride (CaF_2), also called fluorite, is one of the most abundant natural materials and is often present in the ceramic and jewelry industries. This natural material was extensively investigated by Okuno [16], Umesido et al. [17], and Sunta et al. [18] for radiation dosimetry applications.

As we can see, the CaF_2 crystal was synthesized using different techniques and doped with different rare earths and transition metals to improve its luminescence properties. Despite the interesting luminescence properties of Ce-doped CaF_2 [19] and Ce- and Dy-doped CaF_2 [20], the study of Ce- and Li-doped CaF_2 has not yet been carried out. Therefore, in this work, we synthesized Ce- and Li-doped CaF_2 crystal to study its TL response to gamma and UV radiation.

2 Materials and Methods

Calcium fluorite doped with 0.3 mol% Ce and 0.6 mol% Li ($\text{CaF}_2:\text{Ce,Li}$) was synthesized by the combustion method. In a beaker with 5 ml of distilled water, stoichiometric amounts of calcium nitrate tetrahydrate ($\text{Ca}(\text{NO}_3)_2 \cdot 4\text{H}_2\text{O}$) as an oxidant and ammonium fluoride (NH_4F) as a fluorine source for the formation of the CaF_2 structure is dissolved. In this same solution, cerium nitrate ($\text{Ce}(\text{NO}_3)_3 \cdot 6\text{H}_2\text{O}$) and lithium oxide (Li_2O) were added as dopant sources. To produce the combustion reaction, we added urea ($\text{CO}(\text{NH}_2)_2$). The mixture of the reagents dissolved in distilled water was homogenized with a magnetic stirrer at an assisted temperature of 50 °C for 30 min. The beaker is then placed in a muffle furnace maintained at 550 ± 10 °C. The reaction mixture undergoes thermal dehydration and ignites at one point with the release of gaseous products such as nitrogen and carbon oxides. The combustion propagates throughout the reaction mixture. After the combustion process, the crucible and the

synthesized sample were removed from the furnace for rapid cooling. This synthesized sample was sieved to select grains smaller than 0.075 mm in diameter for structural and morphological analysis and pellet production.

To identify the crystalline structure of the synthesized sample, a Rigaku MiniFlex 600 powder diffractometer at 40 kV voltage and 15 mA with $\text{Cu K}\alpha$ -radiation was used. The XRD measurements were taken at the interval of Bragg angle 2θ ($20^\circ \leq 2\theta \leq 80^\circ$) with 0.005° step size and speed of $4^\circ/\text{min}$ at room temperature. The identification of crystalline phases was performed with Panalytical X'Pert HighScore Plus software.

The morphology analysis of the synthesized phosphor particles was observed by scanning electron microscopy (SEM) using a Jeol microscope model JSM-IT700HR.

The particle size was calculated from the full-width half maximum (FWHM) of the intense peak using Scherer's formula [21].

$$D = \frac{0.9 \cdot \lambda}{\beta \cdot \cos\theta} \quad (1)$$

where D is the particle size, β is FWHM (full-width half maximum), λ is the wavelength of the X-ray source, and θ is the diffraction angle.

To evaluate the TL response of $\text{CaF}_2:\text{Ce,Li}$, 6 mm diameter and 1 mm thick pellets were produced from the fine powder of the synthesized phosphorus by pressing in a stainless steel mold at a pressure of 11 ton/cm² at room temperature, followed by a sintering process. To evaluate the effect of sintering temperature on the phosphorus TL response, five groups of previously compacted $\text{CaF}_2:\text{Ce,Li}$ phosphors were subjected to different sintering temperatures (450, 500, 525, 550, and 575 °C) for 2 h.

The TL glow curve was recorded using a Harshaw model 3500 TL reader in the temperature range of 50 to 400 °C with a heating rate of 4 °C/s. Each point in the glow curve represents an average of five readings.

The 3D TL emission spectrum was obtained using an automated Risø TL/OSL reader, model DA-20. For the detection of TL light at different wavelengths, a monochromator was coupled in front of the photomultiplier tube (PMT) of the Risø TL/OSL reader. The scanning was performed from 250 to 650 nm, with a step of 20 nm.

For gamma irradiation of pellets with doses between 1 and 25 Gy, a ⁶⁰Co Picker source, model Gammatron, with an exposure rate of 0.69 Gy/s was used. This source uses an electronic timer system to control the irradiation time. For the determination of the irradiation dose, the following parameters are considered: irradiation distance, decay correction factor, and dose rate. For the irradiation process, the pellets are placed in acrylic matrices and wrapped in aluminum foil in order to have an electronic equilibrium and avoid the effects of visible light on the luminescence of the material. The samples were irradiated at a distance of 10 cm, aligned with the source axis for homogeneous irradiation.

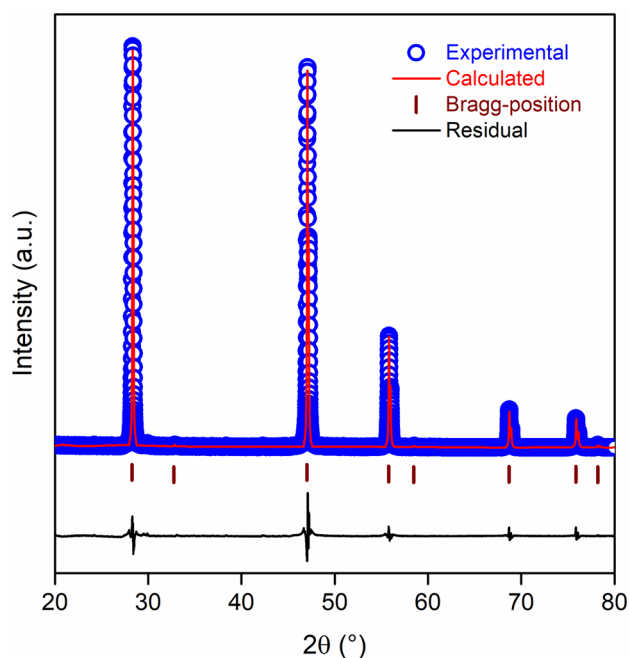


Fig. 1 XRD diffractogram of Ce- and Li-doped CaF_2 phosphor. Experimental (blue open circle), calculated (red solid line), pattern (the brown vertical lines are the Bragg positions), and residual (black solid line)

The pellets were subjected to ultraviolet (UV) irradiation using a 75W XENON ORIEL UV lamp, model 6237. The lamp is located in a dark chamber with a mobile support that allows for varying the distance from the sample to the source. The irradiations have been performed at a constant distance of 14 cm between the sample and the UV light source for time intervals of 5 to 40 s, during which the pellet is placed symmetrically under the UV light source (circular symmetry), ensuring that the entire pellet receives the UV light uniformly. Considering that the penetration of UV light in the sample is superficial, the thermoluminescent reading is performed on the same side that the irradiation of the pellet was performed.

3 Results and Discussion

The powder XRD pattern of phosphor CaF_2 doped with 0.3 mol% Ce and 0.6 mol% Li is shown in Fig. 1 along with its CaF_2 standard file. All the diffraction peaks of the synthesized phosphor agree with the ICDD (International

Centre for Diffraction Data) standard file no. 77–2245, demonstrating that the synthesized sample has a centered cubic phase and space group $\text{Fm}\bar{3}\text{m}$. Therefore, this analysis confirms that the introduction of Ce and Li ions does not interfere with the crystal structure of CaF_2 .

To study the effect of dopant concentration on the lattice parameters of the host, the XRD data were submitted to Rietveld refinement. The function profile used in the Rietveld refinement was a pseudo-Voigt function, with contributions from Gaussian and Lorentzian functions. The Rietveld refinement of the $\text{CaF}_2:\text{Ce},\text{Li}$ phosphor is shown in Fig. 1. Table 1 shows the Rietveld refinement parameters, lattice parameters, volume, and crystallite size of the synthesized phosphor.

The SEM image of the $\text{CaF}_2:\text{Ce},\text{Li}$ sample annealed at 550 °C for 2 h is shown in Fig. 2. This image shows the $\text{CaF}_2:\text{Ce},\text{Li}$ crystallites have an irregular shape and contain some agglomerations of crystallites forming spherical-shaped grains, resulting in larger crystallite sizes, which is in agreement with the XRD results. It was observed that the crystallites are not uniform in shape and size. The non-uniform distribution in shape and size of phosphor may be due to the synthesis temperature during the combustion process.

It is known that the temperature of annealing on samples of $\text{CaF}_2:\text{Mn}$, $\text{CaF}_2:\text{Tm}$, and $\text{CaF}_2:\text{Dy}$ is responsible for the TL sensibility [22].

The efficiency, sensitivity, and dose storage capacity of a new phosphor depend on the structural defect centers grown during the synthesis of the material, and these centers are highly dependent on the type of thermal annealing performed after synthesis. In general, with additional thermal annealing after synthesis, more defects are produced or unstable centers are stabilized, which favors the formation of electron levels or traps responsible for the absorption of the radiation dose. In addition, the production of sensitive dosimeters in the form of pellets by sintering is necessary to find a suitable temperature to obtain sensitive dosimeters with good mechanical resistance for handling. For this purpose, $\text{CaF}_2:\text{Ce},\text{Li}$ phosphor pellets sintered at different temperatures (450, 525, 550, 575, and 600 °C) for 2 h were produced. Figure 3 shows the TL glow curves of $\text{CaF}_2:\text{Ce},\text{Li}$ pellets sintered at different temperatures and exposed to gamma rays at a dose of 3 Gy. Among all, the pellet sintered at 550 °C showed more intense glow peaks. Therefore, the $\text{CaF}_2:\text{Ce},\text{Li}$ phosphor sintered at 550 °C for 2 h was chosen as the optimized phosphor for further TL studies.

Table 1 Rietveld refinement parameters, lattice parameters, volume, and crystalline size of Ce- and Li-doped CaF_2 phosphor

Sample	Refinement parameters			Lattice parameters		Volume (\AA^3)	Crystalline size (nm)
	R_p	R_{wp}	χ^2	$a, b, \text{ and } c$ (\AA)	$\alpha, \beta, \text{ and } \gamma$ ($^\circ$)		
$\text{CaF}_2:\text{Ce},\text{Li}$	12.13	17.13	6.22	5.4653	90	163.24	717.23

Fig. 2 SEM image of $\text{CaF}_2:\text{Ce},\text{Li}$ phosphor annealed at 550°C for 2 hours

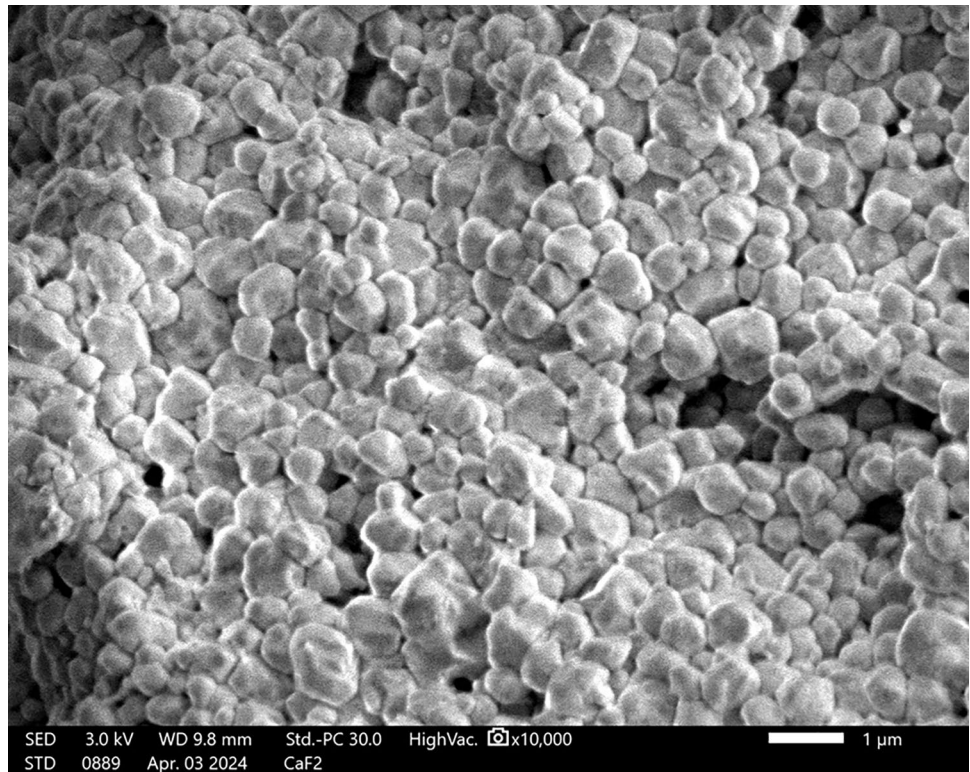


Figure 4 shows the TL glow curve for $\text{CaF}_2:\text{Ce},\text{Li}$ pellets sintered at 550°C for 2 h and irradiated with different doses of gamma radiation from 1 to 25 Gy. Initially, the glow curve shows overlapping peaks, giving rise to two TL peaks centered at 172°C and 275°C . It is observed that the intensity of the TL peak increases with an increasing dose

of at least up to 25 Gy, with no change in the position of the maximum temperature for both peaks. This result evidences that possibly both $\text{CaF}_2:\text{Ce},\text{Li}$ TL peaks obey first-order kinetics (FOK). The inset of Fig. 4 shows the behavior

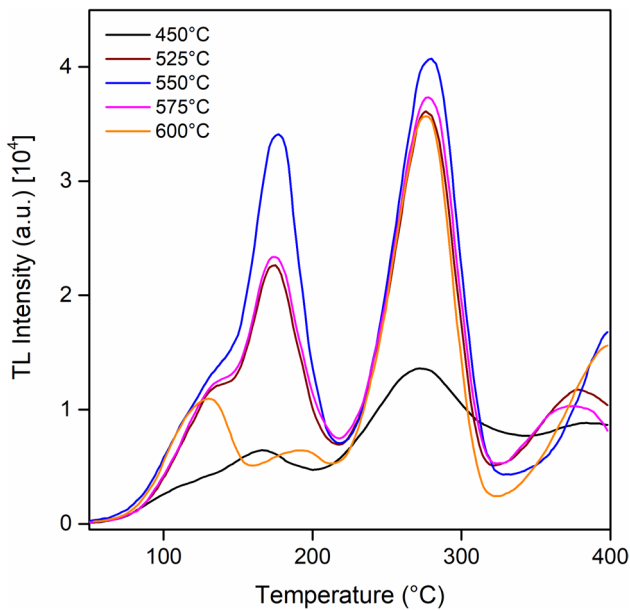


Fig. 3 Effect of sintering temperatures on the TL response of $\text{CaF}_2:\text{Ce},\text{Li}$ pellets (gamma dose = 3 Gy)

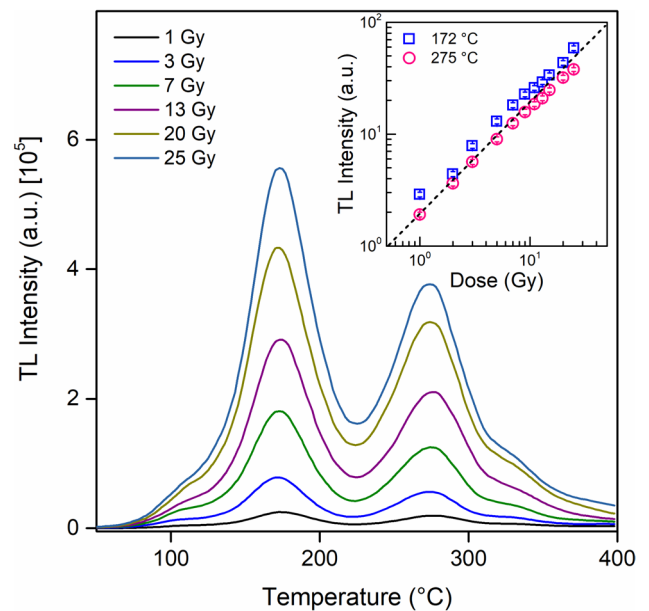


Fig. 4 TL glow curves of the $\text{CaF}_2:\text{Ce},\text{Li}$ pellet irradiated at different gamma-ray doses from 1 to 25 Gy. The inset of the figure shows the behavior of TL intensity as a function of gamma dose for both peaks. The dashed line represents the linear behavior

of TL intensity as a function of gamma dose for $\text{CaF}_2:\text{Ce},\text{Li}$ phosphor. It is observed in the figure that the dose–response shows a linear behavior in the gamma dose region studied.

Recently, Rivera-García et al. [19] studied Ce-doped CaF_2 phosphor and found that the TL glow curve shows an intense peak around 150 °C and an extremely low-intensity peak at 300 °C. On the other hand, Muñoz et al. [23] observed only one intense peak around 123 °C for the Tm-doped CaF_2 sample. Already in our material doped with Ce and Li, in addition to observing the presence of low-temperature peaks similar to the result of Rivera-García et al. [19], we observed the presence of an intense peak at a temperature around 275 °C. Therefore, the presence of the TL peak at 275 °C in the $\text{CaF}_2:\text{Ce},\text{Li}$ phosphor is possibly due to the doping with lithium, since the only difference between the analyzed sample of Rivera-García et al. [19] and the sample analyzed in this work is the doping with Li.

The T_m - T_{stop} [24] and computed glow curve deconvolution (CGCD) [25] methods were used in combination to determine the kinetic parameters of the overlapping peaks in the $\text{CaF}_2:\text{Ce},\text{Li}$ phosphor glow curve.

The T_m - T_{stop} method proposed by McKeever [24] allows for finding the most prominent glow curve peaks. This method generally analyzes glow curves with overlapping peaks, such as $\text{CaF}_2:\text{Ce},\text{Li}$ phosphor. Through the technique, it is possible to obtain information about the order of kinetics and the differences between peaks corresponding to discrete electron traps or those corresponding to a continuous distribution of electron traps [25]. Figure 5 shows the behavior of the results obtained from a T_m - T_{stop} experiment for the T_{stop} temperature between 50 and 300 °C with 10 °C steps.

The invariance of peak position with gamma radiation dose observed in Fig. 4 indicates that the TL glow curve of phosphor $\text{CaF}_2:\text{Ce},\text{Li}$ is formed by the overlapping of peaks with first-order kinetics, except for the TL peak satellite at about 105 °C, which is unstable at room temperature.

From Fig. 5, we can identify four regions: (i) for the region between 50 and 70 °C, a slight increase in T_m is observed, and due to the instability of possible peaks in this region with room temperature, it is not possible to obtain information on the order of kinetics and the distribution (discrete or continuous) of the electron traps; (ii) the second region between 80 to 140 °C presents a slight growth in T_m , and this result indicates the presence of a peak of first-order kinetics of energy levels with continuous distribution; (iii) the third region between 150 to 200 °C shows a slight increase in T_m , indicating first-order kinetics with electron traps of continuous distribution; and (iv) the fourth region between 230 to 300 °C shows an accentuated growth of T_m , which indicates a first-order peak of electron traps with continuous distribution.

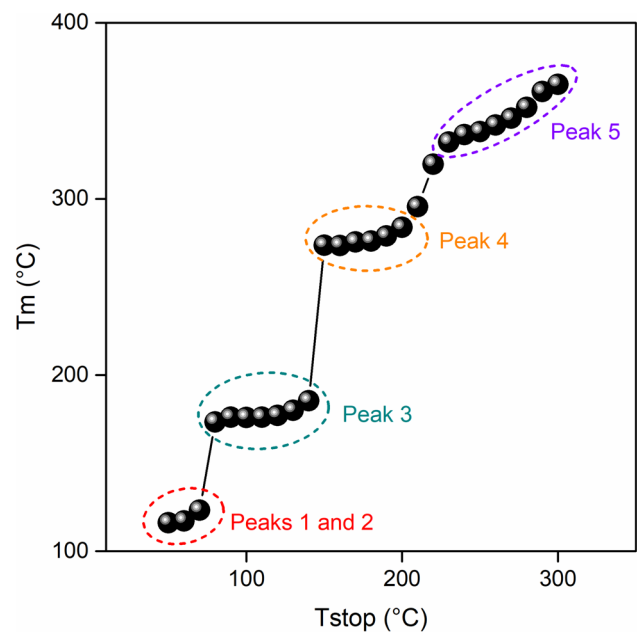


Fig. 5 Variation of maximum peak temperature (T_m) versus T_{stop}

Using the preliminary T_m - T_{stop} results, the deconvolution of the TL glow curve was performed using the computerized glow curve deconvolution (CGCD) method [25]. Figure 6 shows the deconvolution of the TL glow curve of $\text{CaF}_2:\text{Ce},\text{Li}$ phosphors exposed to ^{60}Co gamma rays with doses of 3, 7, and 13 Gy. The kinetic parameters, such as activation energy, kinetic order, and frequency factor of each TL peak, were determined using this method. As seen in this figure, the glow curve contains five overlapping peaks at temperatures of 108, 141, 165, 270, and 317 °C. The FOM value [26] with values less than 3.49 shows a good fit to the experimental glow curve. The kinetic parameters for each TL peak of this irradiated material exposed to gamma doses of 3, 7, and 13 Gy are shown in Tables 2 and 3.

The 3D TL emission spectrum of $\text{CaF}_2:\text{Ce},\text{Li}$ phosphor is shown in Fig. 7. The X coordinate shown in the figure corresponds to the temperature; the Y coordinate corresponds to the TL light emission wavelength, and Z is the TL intensity. The 3D TL emission spectrum can be useful for identifying the types of emission centers and understanding the charge transfer mechanisms that give rise to TL light; moreover, they can provide new information for TL material characterization.

As shown in Fig. 7, the 3D TL emission spectrum of $\text{CaF}_2:\text{Ce},\text{Li}$ phosphor shows the temperature of two peaks centered at 172 and 275 °C and TL peak satellites at 105 and 340 °C. Also, the 3D TL spectrum shows a TL light emission band with a wavelength between 320 and 460 nm centered at 380 nm, which corresponds to the recombination transitions of the released electrons coming from the electron levels or traps. Therefore, we can affirm that there are possibly several electron traps and a single recombination center that participate during TL light emission.

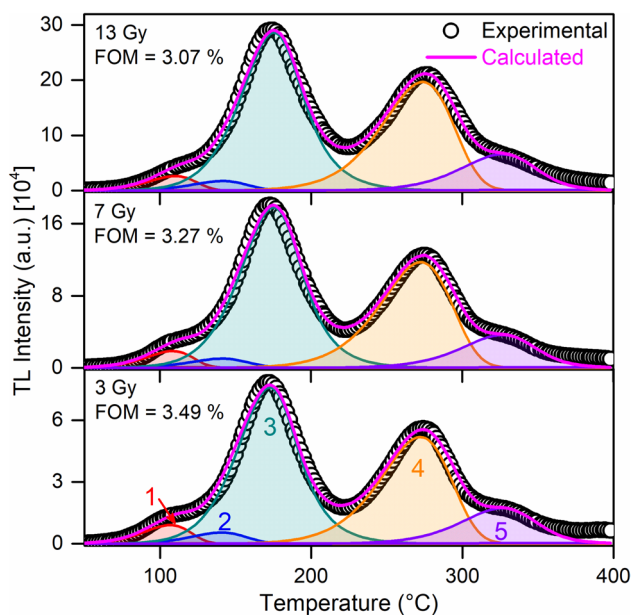


Fig. 6 Deconvoluted TL glow curves of Ce- and Li-doped CaF₂ phosphor irradiated with gamma doses of 3, 7, and 13 Gy

The effect of UV radiation on CaF₂:Ce,Li pellets synthesized at different temperatures was also investigated to obtain the best response in their TL glow curve. From Fig. 8, we can observe that, in general, the intensity of the glow curves decreases with increasing sintering temperature. Despite observing a more intense TL response for a heat treatment of 450 °C, the pellets sintered at 525 °C present two peaks centered at 195 and 280 °C, the second peak being more intense. Therefore, we proceeded to study the effect of UV exposure time on these samples.

The effect of UV exposure time on the TL glow curve of the sintered pellets at 525 °C for 2 h was studied. The TL glow curve was recorded using a UV exposure time of 5 to 90 s, recording the glow curves with a heating rate of 4 °C/s (Fig. 9). It was observed that the TL intensity of both TL peaks increased with increasing UV exposure time up to 90 s. The UV exposure time does not affect the position of the second peak. However, the position of the first peak undergoes a slight shift at high temperatures for exposure times above 30 s. In the inset of Fig. 9, it is observed that the TL intensity of both peaks grows sub-linearly with UV exposure time.

For both types of radiation (gamma and UV), the TL glow curve of CaF₂:Ce,Li presents completely dislocated peaks, except for the peak at about 275 °C. The low-temperature peak is more intense in the sample irradiated with UV light. In addition, the peaks induced by UV light are broader, possibly due to the superposition of several TL peaks. These changes in peak positions and TL intensities are observed due to variations in the

Table 2 Details of activation energy (*E*), maximum temperature (*T*), distribution width (σ), and frequency factors (*s*) of the TL peaks 1, 2, and 3 of the CaF₂:Ce,Li phosphor obtained by the deconvolution method of the glow curves for different doses. Bottom: the average

Dose (Gy)	FOM (%)	Peak 1: FOK—discrete			Peak 2: GOK—discrete			Peak 3: FOK—continuous			
		<i>E</i> (eV)	<i>T</i> (°C)	<i>s</i> (s ⁻¹)	<i>E</i> (eV)	<i>T</i> (°C)	<i>s</i> (s ⁻¹)	<i>E</i> (eV)	σ (eV)	<i>T</i> (°C)	<i>s</i> (s ⁻¹)
3	3.49	0.776	106.60	4.89 × 10 ⁹	0.83	140.73	3.23 × 10 ⁹	0.94	0.036	163.08	1.70 × 10 ¹⁰
7	3.27	0.796	108.51	8.22 × 10 ⁹	0.81	141.23	1.45 × 10 ⁹	0.93	0.035	165.68	1.19 × 10 ¹⁰
13	3.07	0.776	110.14	3.86 × 10 ⁹	0.83	141.39	3.10 × 10 ⁹	0.94	0.038	165.57	1.46 × 10 ¹⁰
Average		0.78 (7)	108.4 (9)	5.66 (3) × 10 ⁹	0.83 (8)	141.1 (4)	2.59 (2) × 10 ⁹	0.94 (4)	0.04 (2)	164.8 (8)	1.45 (3) × 10 ¹⁰

Table 3 Details of activation energy (E), maximum temperature (T), distribution width (σ), and frequency factors (s) of the TL peaks 4 and 5 of the $\text{CaF}_2:\text{Ce},\text{Li}$ phosphor obtained by the deconvolution method of the glow curves for different doses. Bottom: the average

Dose (Gy)	FOM (%)	Peak 4: FOK—continuous				Peak 5: FOK—continuous			
		E (eV)	σ (eV)	T ($^{\circ}\text{C}$)	s (s^{-1})	E (eV)	σ (eV)	T ($^{\circ}\text{C}$)	s (s^{-1})
3	3.49	1.08	0.0087	268.57	1.99×10^9	1.31	0.031	316.99	2.54×10^{10}
7	3.27	1.08	0.0087	269.01	1.80×10^9	1.33	0.031	317.27	4.15×10^9
13	3.07	1.08	0.0087	270.02	1.86×10^9	1.31	0.031	316.97	2.54×10^{10}
Average		1.08 (3)	0.009 (2)	269.2 (6)	$1.89 (6) \times 10^9$	1.32 (8)	0.03 (1)	317.08 (3)	$3.08 (6) \times 10^{10}$

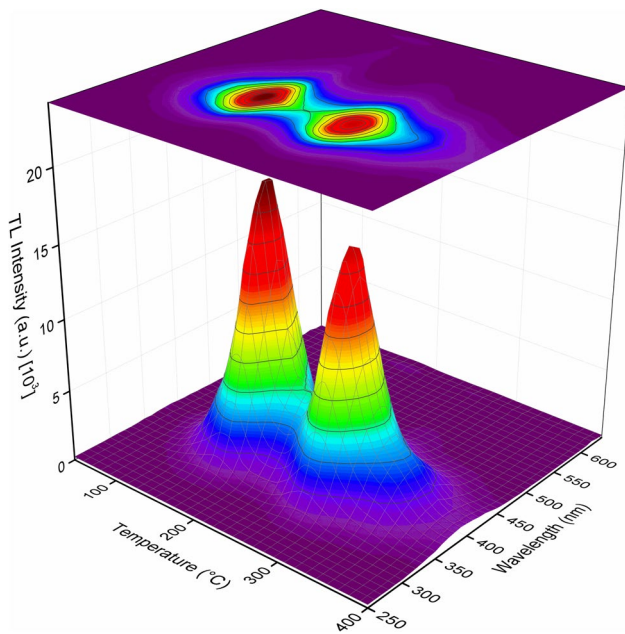


Fig. 7 3D TL emission spectrum of $\text{CaF}_2:\text{Ce},\text{Li}$ phosphor. The sample was exposed to 10 Gy gamma radiation at room temperature

population of electrons trapped in trapping centers. With UV light irradiation, there is higher electron trapping in shallow traps (lower temperature peaks), and with gamma

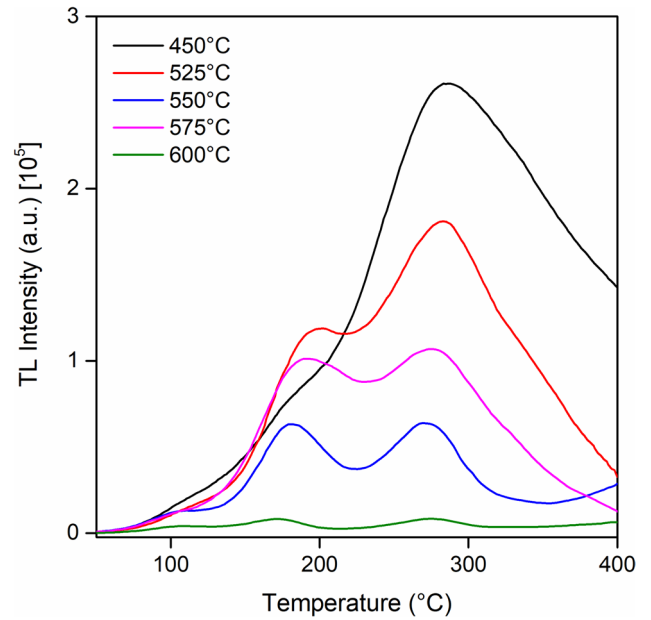


Fig. 8 CaF_2 pellets sintering to different temperatures and irradiated with a UV source for 20 seconds

irradiation, the TL peak at 275 $^{\circ}\text{C}$ increases relative to the other peaks, representing higher electron trapping in deep traps. A similar behavior was observed by de la Rosa-Cruz et al. [27] in a sample of zirconium oxide doped with rare earths.

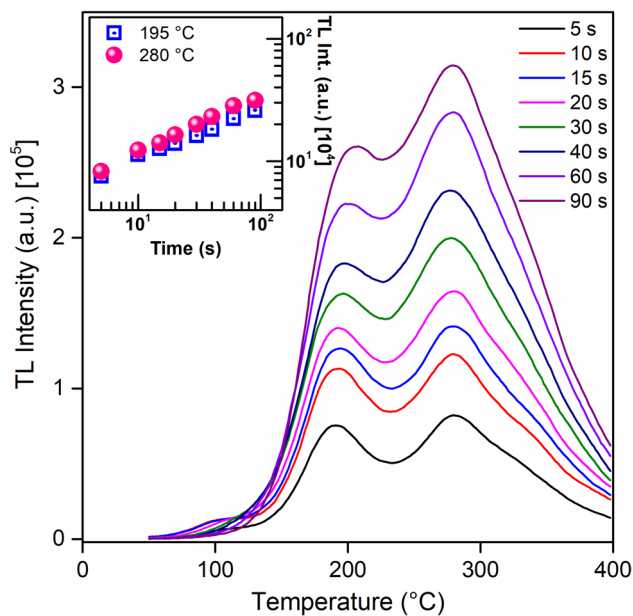


Fig. 9 TL curve of $\text{CaF}_2\text{:Ce,Li}$ to different times of irradiation of UV source. In the inset of the figure, TL intensity for different times of UV irradiation

4 Conclusions

In conclusion, Ce- and Li-doped CaF_2 phosphor has been successfully produced using the combustion synthesis route. A structural study of the $\text{CaF}_2\text{:Ce,Li}$ phosphor by XRD shows a centered cubic phase structure and $\text{Fm}3\text{m}$ space group with a crystallite size of 717 nm. SEM images also confirmed this crystallite size. Pellets sintered at 550°C show the best TL response when exposed to gamma radiation, with two peaks centered at 172 and 275°C . On the other hand, pellets sintered at 525°C presented a good TL response for UV radiation, with two main peaks centered at 195 and 280°C . The TL intensity of the peaks centered at 172 and 275°C grows linearly with increasing gamma radiation doses between 1 and 25 Gy. However, the behavior of TL intensity with UV exposure time is sublinear. Combined analysis using the T_m - T_{stop} and deconvolution methods showed that the glow curve exhibits five TL peaks. The TL emission spectrum showed the presence of a recombination center emitting TL light with a wavelength of 380 nm.

Acknowledgements The authors would like to thank the “Central de Analises Multiusuário” laboratory of IPEN/CNEN-SP for the SEM measurements.

Author Contributions N.F. Cano, J. Mosqueira-Yauri and J.S. Ayala-Arenas conceived the idea developed, supervised the work, verified the results, and writing of original draft. R.R.M. Acquapucho, J.F.D. Chubaci and René R. Rocca performed the TL measurements. K. V. Turpo H. performed the analysis of the XRD measurements. L.M. Rondan-Flores performed the SEM measurements and image analysis.

J.F. Benavente performed the theoretical deconvolution analysis of the TL glow curves. All authors discussed the results and contributed to the final manuscript.

Funding This work was supported by PROCENCIA-CONCYTEC, Peru, in the framework of the call E041-2022-1 (Process number N° PE501078121-2022-PROCENCIA).

Data Availability No datasets were generated or analysed during the current study.

Declarations

Competing Interests The authors declare no competing interests.

References

- E.G. Yukihara, S.W.S. McKeever, C.E. Andersen, A.J.J. Bos, I.K. Bailiff, E.M. Yoshimura, G.O. Sawakuchi, L. Bossin, J.B. Christensen, Luminescence dosimetry. *Nat. Rev. Methods Primers* **2**, 26 (2022). <https://doi.org/10.1038/s43586-022-00102-0>
- H. Yazan, Z.G. Portakal-Uçar, S. Akça, M. Topaksu, P.D. Townsend, N. Can, Thermoluminescence of Ce and Nd codoped CaF_2 phosphors after beta irradiation. *J. Lumin.* **234**, 117949 (2021). <https://doi.org/10.1016/j.jlumin.2021.117949>
- A. Zarate-Morales, A.E. Buenfil, Environmental gamma dose measurements in Mexico City using TLD. *Health Phys.* **71**, 358–361 (1996)
- M. Zahedifar, E. Sadeghi, S. Harooni, Thermoluminescence characteristics of the novel $\text{CaF}_2\text{:Dy}$ nanoparticles prepared by using the hydrothermal method. *Nucl. Instrum. Meth. B* **291**, 65–72 (2012). <https://doi.org/10.1016/j.nimb.2012.09.013>
- M. Zahedifar, E. Sadeghi, Z. Mohebbi, Synthesis and thermoluminescence characteristics of Mn doped CaF_2 nanoparticles. *Nucl. Instrum. Meth. B* **274**, 162–166 (2012). <https://doi.org/10.1016/j.nimb.2011.12.015>
- M. Zahedifar, E. Sadeghi, Thermoluminescence dosimetry properties of new Cu doped CaF_2 nanoparticles. *Radiat. Prot. Dosim.* **157**, 303–309 (2013). <https://doi.org/10.1093/rpd/nct151>
- S. Masilla Moses Kennedy, Thermoluminescence studies on γ -irradiated $\text{CaF}_2\text{:Dy:Pb:Na}$ single crystals. *J. Rare Earth* **27**, 187–191 (2009). [https://doi.org/10.1016/S1002-0721\(08\)60217-3](https://doi.org/10.1016/S1002-0721(08)60217-3)
- D.A.A. Vasconcelos, V.S.M. Barros, H.J. Khoury, W.M. Azevedo, V.K. Asfora, P.L. Guzzo, Synthesis and thermoluminescent response of CaF_2 doped with Tm^{3+} . *Radiat. Meas.* **71**, 51–54 (2014). <https://doi.org/10.1016/j.radmeas.2014.05.027>
- A.N. Yazici, R. Chen, S. Solak, Z. Yegingil, The analysis of thermoluminescent glow peaks of $\text{CaF}_2\text{:Dy}$ (TLD-200) after β -irradiation. *J. Phys. D Appl. Phys.* **35**, 2526 (2002). <https://doi.org/10.1088/0022-3727/35/20/311>
- A.N. Yazici, M. Bedir, A.S. Sökücü, The analysis of dosimetric thermoluminescent glow peak of $\text{CaF}_2\text{:Mn}$ after β -irradiation. *Nucl. Instrum. Meth. B* **259**, 955–965 (2007). <https://doi.org/10.1016/j.nimb.2007.02.104>
- M. Topaksu, A.N. Yazici, The thermoluminescence properties of natural CaF_2 after β -irradiation. *Nucl. Instrum. Meth. B* **264**, 293–301 (2007). <https://doi.org/10.1016/j.nimb.2007.09.018>
- M. Pietriková, L. Krása, L. Juha, Thermoluminescence glow curves of $\text{CaF}_2\text{:Dy}$ crystals irradiated by soft X-rays. *Z. Phys. B Condens. Matter* **93**, 63–66 (1993). <https://doi.org/10.1007/BF01308808>
- H.C. Wulf, M. Gniadecka, $\text{CaF}_2\text{:Dy}$ and $\text{CaF}_2\text{:Ce}$ crystal-based UV dosimeters. *Skin Res. Technol.* **2**, 108–113 (1996). <https://doi.org/10.1111/j.1600-0846.1996.tb00071.x>

14. M. Topaksu, V. Correcher, J. Garcia-Guinea, Luminescence emission of natural fluorite and synthetic $\text{CaF}_2:\text{Mn}$ (TLD-400). *Radiat. Phys. Chem.* **119**, 151–156 (2016). <https://doi.org/10.1016/j.radphyschem.2015.10.002>
15. M.S. Bhadane, K. Hareesh, S.S. Dahiwal, K.R. Sature, B.J. Patil, K. Asokan, D. Kanjilal, V.N. Bhoraskar, S.D. Dhole, A highly sensitive $\text{CaF}_2:\text{Dy}$ nanophosphor as an efficient low energy ion dosimetry. *Nucl. Instrum. Meth. B* **386**, 61–69 (2016). <https://doi.org/10.1016/j.nimb.2016.09.017>
16. E. Emico, S. Watanabe, U.V. induced thermoluminescence on natural calcium fluoride. *Health Phys.* **23**, 377–382 (1972)
17. N.K. Umisedo, E. Okuno, F. Cancio, E.M. Yoshimura, R. Künzel, Development of a mechanically resistant fluorite-based pellet to be used in personal dosimetry. *Radiat. Meas.* **134**, 106330 (2020). <https://doi.org/10.1016/j.radmeas.2020.106330>
18. C.M. Sunta, E.M. Yoshimura, E. Okuno, Sensitization and supra-linearity of CaF_2 : natural thermoluminescent phosphor. Interpretation based on partially interactive traps. *Phys. Status Solidi a* **142** (1994) 253–264. <https://doi.org/10.1002/pssa.2211420128>
19. J.A. Rivera-García, J. Mosqueira-Yauri, T.K. Gundu Rao, E.A. Canaza-Mamani, G.G. Fiorini, J.F. Benavente, C.D. Gonzales-Lorenzo, J.F.D. Chubaci, S. Watanabe, J.S. Ayala-Arenas, N.F. Cano, Synthesis and thermoluminescence of Ce-doped CaF_2 phosphor: study of defect centers responsible for the TL emission by EPR analysis. *J. Lumin.* **261**, 119906 (2023). <https://doi.org/10.1016/j.jlumin.2023.119906>
20. P.R. González, D. Mendoza-Anaya, L. Mendoza, L. Escobar-Alarcón, Luminescence and dosimetric properties of $\text{CaF}_2:\text{Ce}$, Dy phosphor. *J. Lumin.* **195**, 321–325 (2018). <https://doi.org/10.1016/j.jlumin.2017.11.050>
21. B.D. Cullity, S.R. Stock, *Elements of X-ray diffraction*, 3rd edn. (Prentice Hall, New Jersey, 2001), p. 170
22. V.E. Kafadar, A.N. Yazici, R.G. Yildirim, The effects of heating rate on the dose response characteristics of TLD-200, TLD-300 and TLD-400. *Nucl. Instrum. Meth. B* **267**, 3337–3346 (2009). <https://doi.org/10.1016/j.nimb.2009.06.114>
23. I.D. Muñoz, O. Avila, I. Gamboa-deBuen, M.E. Brandan, Evolution of the $\text{CaF}_2:\text{Tm}$ (TLD-300) glow curve as an indicator of beam quality for low-energy photon beams. *Phys. Med. Biol.* **60**, 2135–2144 (2015). <https://doi.org/10.1088/0031-9155/60/6/2135>
24. S.W.S. McKeever, *Thermoluminescence of solids* (Cambridge University Press, London, 1985)
25. J.F. Benavente, J.M. Gómez-Ros, A.M. Romero, Thermoluminescence glow curve deconvolution for discrete and continuous trap distributions. *Appl. Radiat. Isot.* **153**, 108843 (2019). <https://doi.org/10.1016/j.apradiso.2019.108843>
26. H.G. Balian, N.W. Eddy, Figure of merit (FOM), an improved criterion over the normalised chi-squared test for assessing goodness-of-fit of gamma ray spectra peaks. *Nucl. Instrum. Methods* **145**, 389–395 (1977). [https://doi.org/10.1016/0029-554X\(77\)90437-2](https://doi.org/10.1016/0029-554X(77)90437-2)
27. E. de la Rosa-Cruz, L.A. Díaz-Torres, P. Salas, D. Mendoza, J.M. Hernández, V.M. Castaño, Luminescence and thermoluminescence induced by gamma and UV-irradiation in pure and rare earth doped zirconium oxide. *Opt. Mater.* **19**, 195–199 (2002). [https://doi.org/10.1016/S0925-3467\(01\)00219-1](https://doi.org/10.1016/S0925-3467(01)00219-1)

Publisher's Note Springer Nature remains neutral with regard to jurisdictional claims in published maps and institutional affiliations.

Springer Nature or its licensor (e.g. a society or other partner) holds exclusive rights to this article under a publishing agreement with the author(s) or other rightsholder(s); author self-archiving of the accepted manuscript version of this article is solely governed by the terms of such publishing agreement and applicable law.